# Quantum-Mechanical Calculations of Charge Transfer Cross Sections in Collisions of $O^{3+}$ with He

Yong Wu and Jian-guo Wang

Institute of Applied physics and Computational mathematics, China

NIFS, 2008.12

## Our group:

**Prof. Jianguo Wang**

**Bin He, Yong Wu, Ling Liu**

**Research Interest:** **Heavy particle collisions in the whole energy region.**

## Theoretical methods:

**Quantum-mechanical molecular-orbital close-coupling (QMOCC) : ⩽ 5keV/u; Atomic-orbital close-coupling (AOCC): $10^0$ keV/u ~ $10^2$keV/u; Classical-trajectory Monte-Carlo (CTMC): ⩾ $10^1$keV/u**

**Semi-classical molecular-orbital close-coupling method (SCMOCC); MCLZ.**

# *Outline*

- Background
- Theoretical methods
- **Results and discussion**
- Summary and perspectives

# Charge transfer process

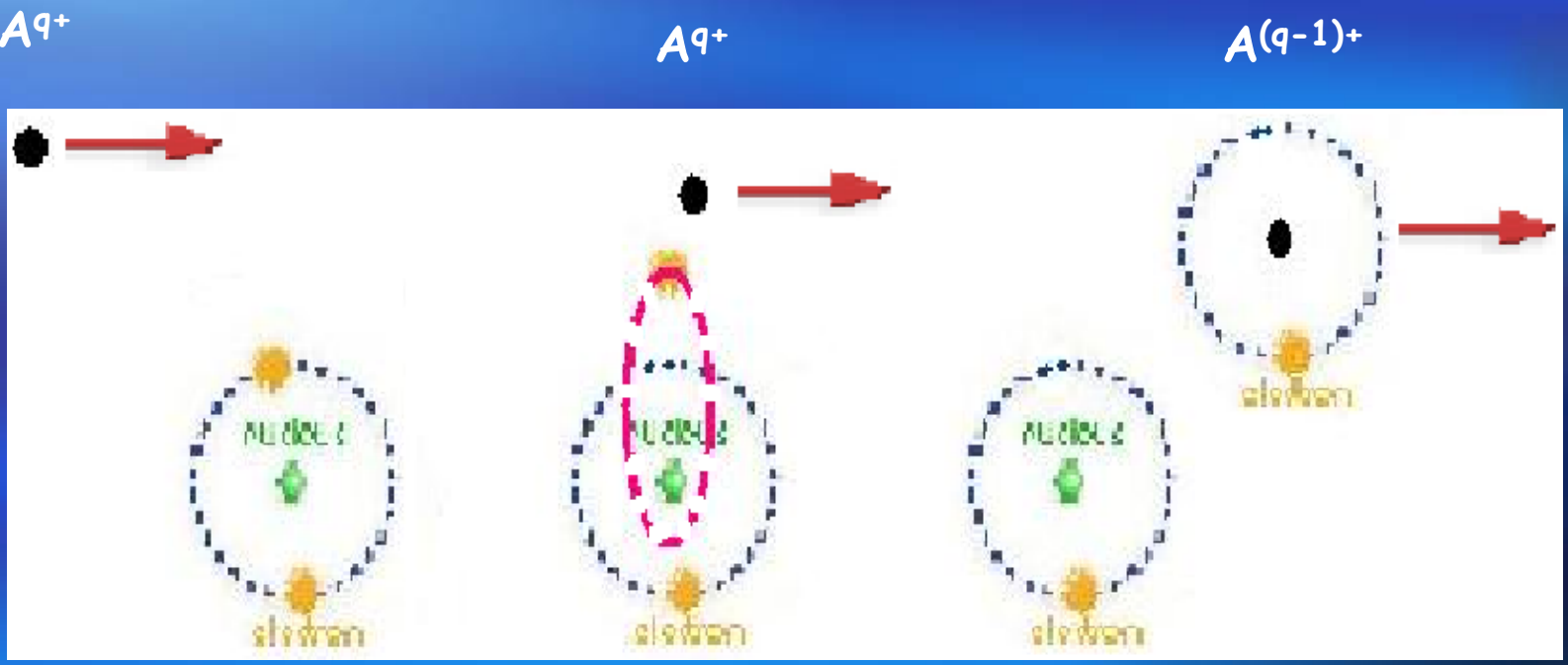

# Background

## 1, Fundamental investigation

Understanding of collision dynamics of many-center and many-electron systems and investigating the electron correlation effects.

## 2, Applications in astrophysics and plasma physics

In the environment of some lab plasma or astrophysics, for the low energy or low density of electron, reaction by heavy particle collisions dominate.

Divertor region, Neutral beam injection, EUV and X-ray in comet and planetary atmospheres.

All kinds of cross section and rate coefficient are needed.

However, these data are still not enough.

# EUV and Soft X-ray

Solar wind: $O^{q+}$,$S^{q+}$,$Ne^{q+}$,…; planet and comet atmosphere

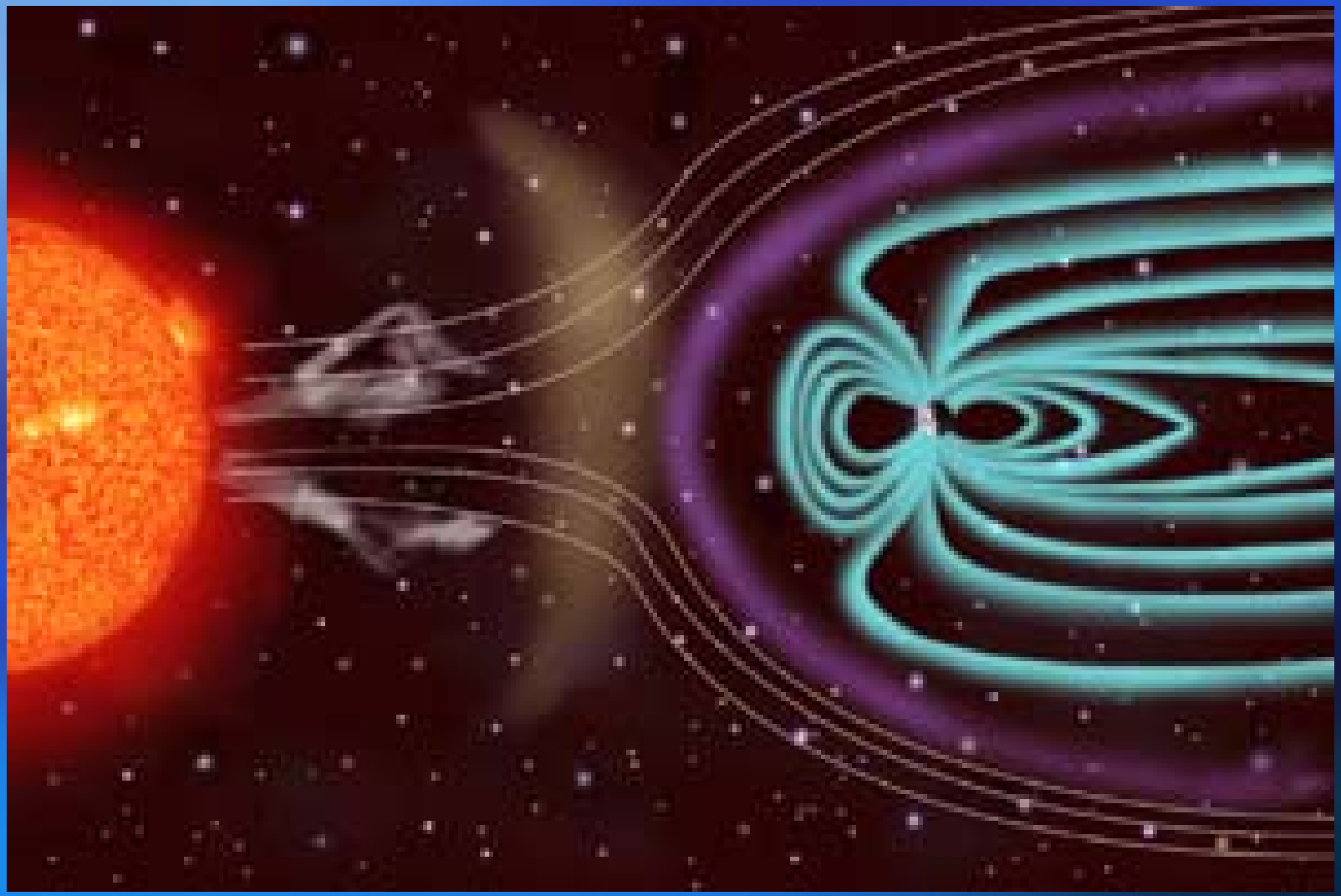

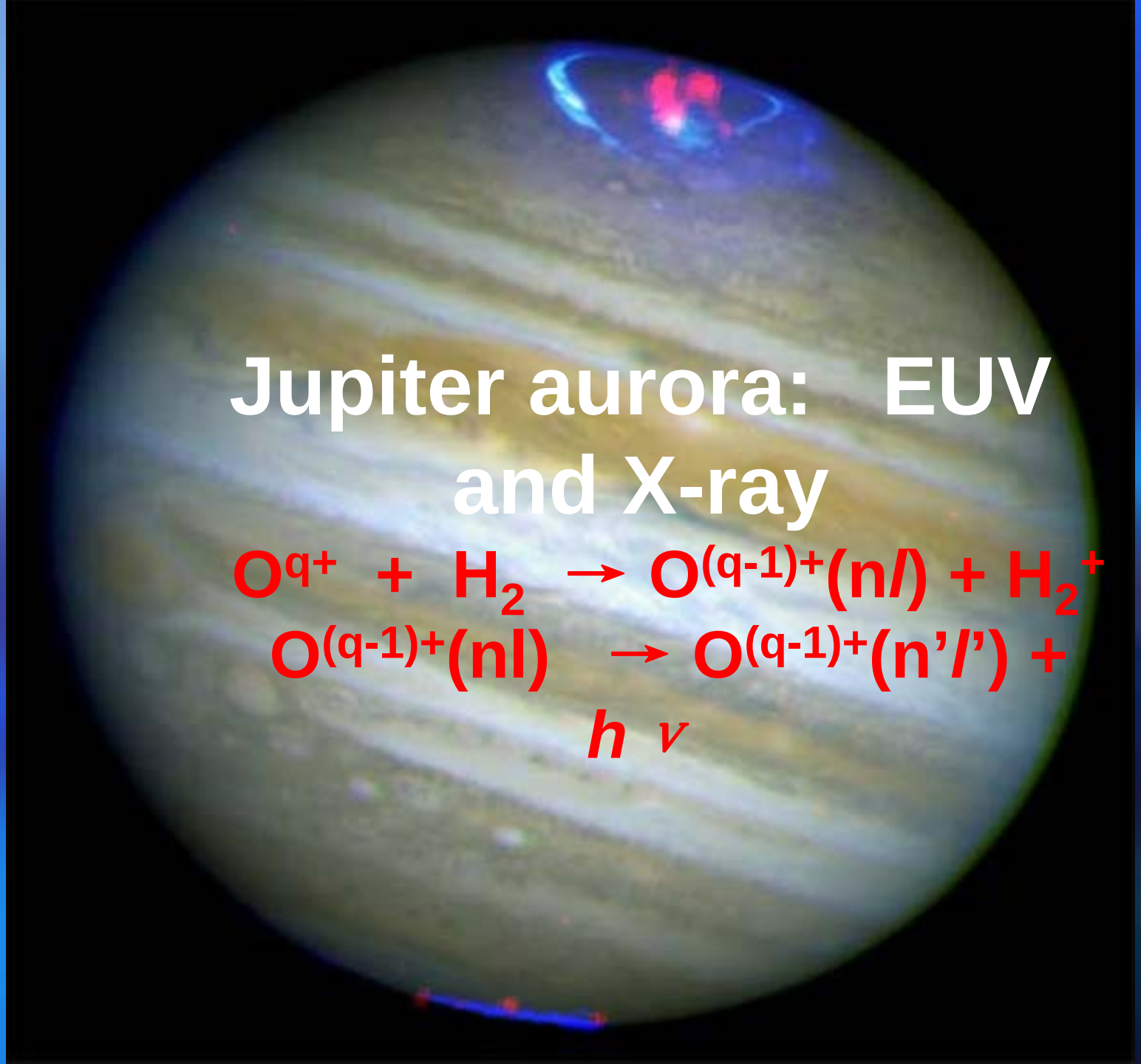
Jupiter aurora: EUV and X-ray
$O^{q+} + H_2 \rightarrow O^{(q-1)+}(nl) + H_2^+$
$O^{(q-1)+}(nl) \rightarrow O^{(q-1)+}(n'l') + h\nu$

# Magnetic Confinement Fusion (ITER)

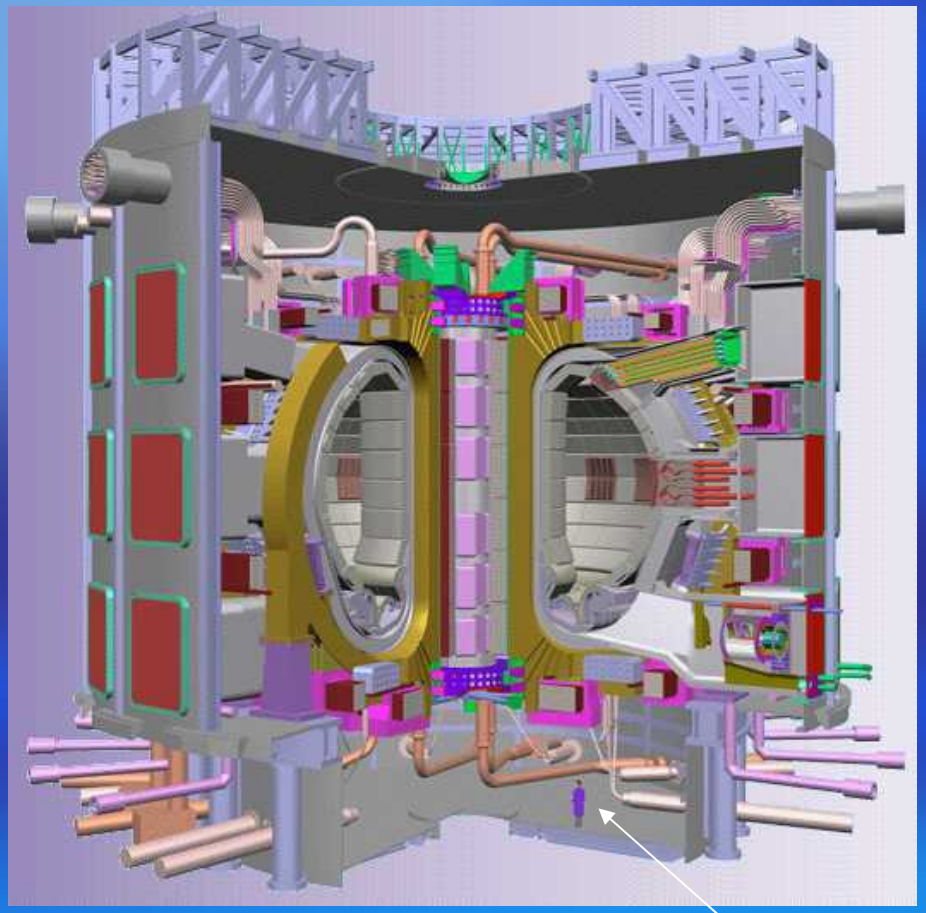


**Diagnosing of impurities by neutral beam injection**

**Divertor Region of a Tokamak Fusion Device**

# Theoretical Methods

**(1) Electron Structure Calculation of small molecules:**

**Multi-reference single- and double-excitation configuration interaction approach (MRDCI)**

High excited states

CI: solving a secular equation, large number of configurations

Group theory: Truncate the CI basis; MO: symmetry orbitals, transform according to the irreducible representations (IRs) of the molecular point group; Block the Hamiltonian matrices.

Configurations selection: threshold $10^{-8}$ Hartree; contributions from the unselected configurations are considered by employing an extrapolation procedure.

# Introduction of MOCC

## (2) Scattering Theory:

**Fully quantum mechanical molecular orbital close-coupling (MOCC)**

**Approximations:**
**Born-Oppenheim approximation (BO):**
**Fixed-nuclei approximation, decomposing the motions of nucleus and electrons.**
**Perturbed stationary-state approximation (PSS)**

$$\psi\ (R, \rho_i) = \sum_{\gamma}\ F_{\gamma}(R)\phi_{\gamma}(\rho_i \mid R)$$

# Introduction of MOCC

**System Hamilton:**

$$H\ (R, \rho_i) = -\frac{1}{2\mu_R}\nabla_R^2 + H_{ad}\ (\rho_i \mid R) \qquad (1)$$

**where $H_{ad}$ is the adiabatic Hamilton and the corresponding Schrödinger equations are given as follow:**

$$H_{ad}(\rho_i \mid R)\phi_\gamma(\rho_i \mid R) = \varepsilon_\gamma(R,)\phi_\gamma(\rho_i \mid R) \qquad (2)$$

# Introduction of MOCC

**Using the perturbed stationary-state (PSS) approximation, the total wave function can be represented as:**

$$\psi\ (R, \rho_i) = \sum_{\gamma} F_{\gamma}(R)\phi_{\gamma}(\rho_i \mid R) \qquad (3)$$

**By the variation theory, the adiabatic close-coupling scattering equation is obtained:**

$$\left(-\frac{1}{2\mu}\nabla_R^2\vec{\mathrm{I}} - \vec{\epsilon}(R) + E\vec{\mathrm{I}} + \frac{1}{2\mu}\left[2\vec{\mathrm{A}}(\vec{\mathrm{R}})\cdot\nabla_R + \vec{\mathrm{B}}(\vec{\mathrm{R}})\right]\right) F^a(\vec{\mathrm{R}}) = 0$$

**Where**

$$\vec{\mathrm{A}}(\vec{\mathrm{R}})_{ij} = \langle\psi_i^a \mid \nabla_R \mid \psi_j^a\rangle$$
$$\vec{\mathrm{B}}(\vec{\mathrm{R}})_{ij} = \langle\psi_i^a \mid \nabla_R^2 \mid \psi_j^a\rangle$$

**are radial coupling matrixes.**

# Introduction of MOCC

**For the convenience of numerical solution, the coupled equations are transformed to a diabatic representation:**

$$\left\{\nabla_R^2 + 2\mu_R\left[E - \varepsilon_\gamma^d(R,\theta)\right]\right\}F_\gamma(R,\theta) = 2\mu_R\sum_{\gamma'\neq\gamma}V_{\gamma,\gamma'}^d F_{\gamma'}(R,\theta) \qquad (4)$$

**Where** $\vec{\mathbf{V}}(R) = \vec{\mathbf{C}}^{-1}(R)\vec{\epsilon}(R)\vec{\mathbf{C}}(R)$ **, and** $C$ **is the transformation matrix:** $\frac{d\vec{\mathbf{C}}}{dR} + \vec{\mathbf{A}}\vec{\mathbf{C}} = 0$ **;** $\varepsilon_\gamma^{\,d}(R)$ **is the diabatic potential curves; and** $V_{\gamma,\gamma'}^d(R)$ **is the diabatic coupled radial matrix element.**

# Introduction of MOCC

**Using the parital-wave decomposition method, with the plane wave boundary conditions at a large internuclear distance, the diabatic close-coupling scattering equations are solved and the radial wavefunction and the S-matrix are obtained:**

$$\lim_{R\to\infty} f_{\gamma}^{lm}(R) \to \frac{1}{\sqrt{k_{\gamma'}}}\{\delta_{\gamma,\gamma'} j_l(k_{\gamma}R) + K^{l}_{\gamma,\gamma'}\eta_l(k_{\gamma'}R)\}$$

$$S^{l} = \frac{I + iK^{l}}{I - iK^{l}} \qquad (5)$$

# Introduction of MOCC

**The differential and integral total cross sections are respectively:**

$$\frac{d\sigma(\theta)}{d\Omega} = \frac{1}{4k^2}\left[\sum_l (2l+1) S^l_{i,j} P_l(\cos\theta)\right]^2, \qquad (6)$$

$$\sigma_{tot}(k) = \frac{\pi}{k_i^2}\sum_l (2l+1)\left(\left|\delta_{ij} - S^l\right|^2_{i,j}\right) \qquad (7)$$

# Results and discussions

## The reaction studied:

$$O^{3+}(2s^2 2p\ ^2P^o) + He(1s^2\ ^1S) \rightarrow O^{2+} + He^{+}\ (O^{+} + He^{2+})$$

**A series of measurements reported recently: Kamber [PRA 77, 012701 (2008)], Ishii [PRA 70 042716 (2004)], Bangsgaard[1989 Phys. Scr. T28, 91]**

## (Ⅰ) Potentials and Radial Couplings (MRDCI)

**Symmetry:** $^2\Sigma^+$ , $^2\Pi$

**Basis set: the Cartesian Gaussian type**

**O: (21s,6p,3d,2f) contracted to (5s,4p,3d,2f)**

**diffuse basis set(2s,2p,2d)**

**He: (6s,2p,1d) contracted to (3s,2p,1d)**

**diffuse basis set(1s, 1p, 1d)**

**Configurations: threshold $10^{-9}$ Hartree**

**numbers:** $^2\Sigma^+$ **~35000,** $^2\Pi$ **~30000**

# Adiabatic potential curves for $(OHe)^{3+}$ system

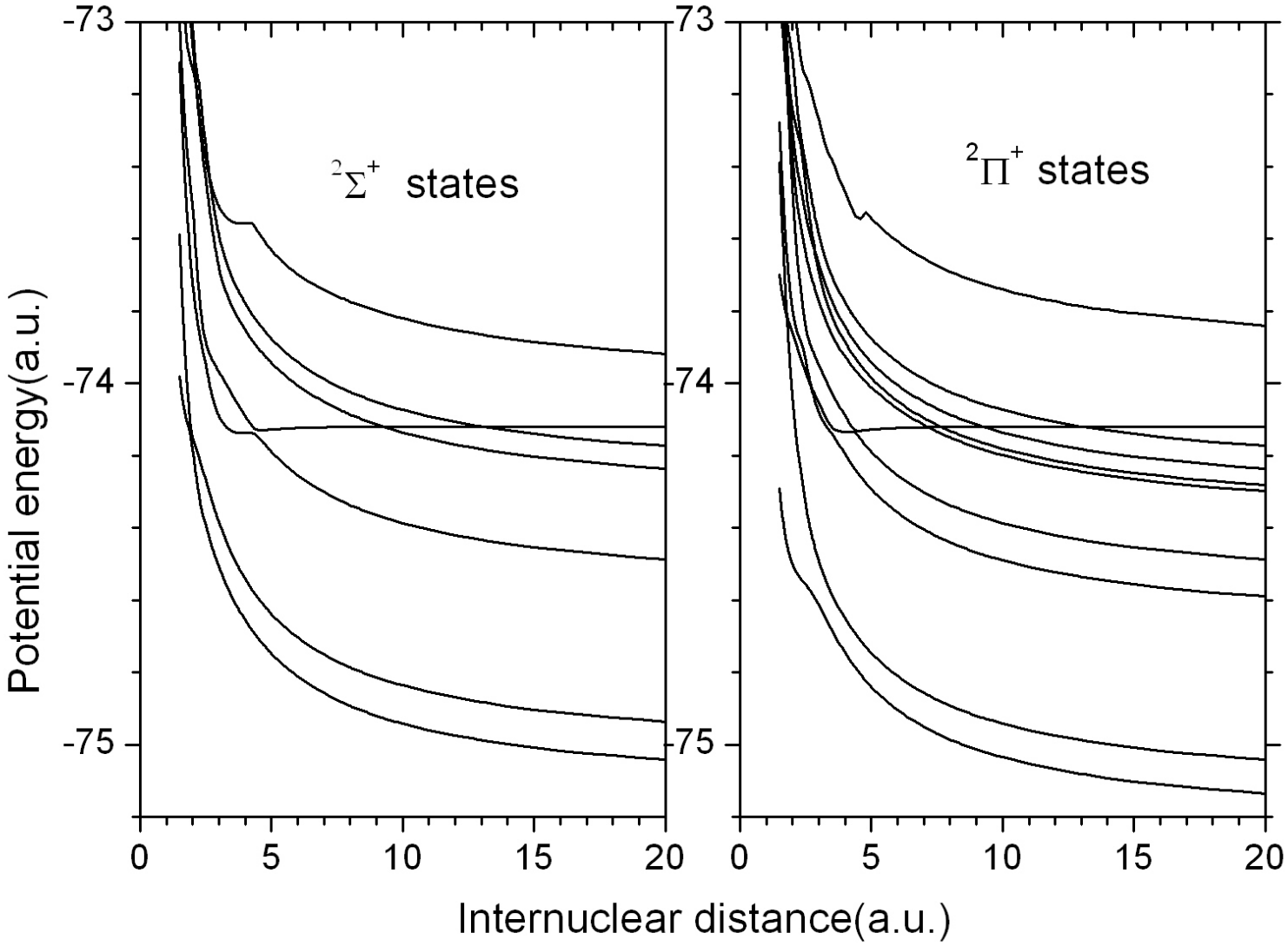

# Comparison of dissociation energies of the $[OHe]^{3+}$ ($^2\Sigma^+$)

| Molecular states | MRDCI results (eV) | Experimental values (eV) [23] | $\Delta E$ (eV) |
|---|---|---|---|
| 1 $^2\Sigma^+[O^{2+}(2s^22p^2\ ^1D)+He^+(1s\ ^2S)]$ | 2.5434 | 2.5136 | 0.0298 |
| 2 $^2\Sigma^+[O^{2+}(\ 2s^22p^2\ ^1S)+He^+\ (1s\ ^2S)]$ | 5.4087 | 5.3544 | 0.0543 |
| 3 $^2\Sigma^+[O^{2+}(\ 2s2p^3\ ^3P^o)+He^+\ (1s\ ^2S)]$ | 17.6373 | 17.6532 | 0.0159 |
| 4 $^2\Sigma^+[O^+(2s^22p^3\ ^2P^o)+He^{2+}\ ]$ | 24.4645 | 24.3140 | 0.1505 |
| 5 $^2\Sigma^+[O^{2+}(\ 2s2p^3\ ^1P^o)+He^+\ (1s\ ^2S)]$ | 26.1609 | 26.0939 | 0.0670 |
| 6 $^2\Sigma^+[O^{3+}(2s^22p\ ^2P^o)+He(1s^2\ ^1S)]$ | 30.3597 | 30.3800 | 0.0203 |
| 7 $^2\Sigma^+[O^{2+}(2s^22p3s\ ^3P^o)+He^+\ (1s\ ^2S)]$ | 33.1247 | 33.1666 | 0.0419 |

# Comparison of dissociation energies of the $[OHe]^{3+}$ ($^2\Pi$)

| Molecular states | MRDCI results (eV) | Experimental values (eV) [23] | $\Delta E$ (eV) |
|---|---|---|---|
| 1 $^2\Pi$ $[O^{2+}(2s^22p^2\ ^3P)+He^+(1s\ ^2S)]$ | 0.0 | 0.02577 | 0.0258 |
| 2 $^2\Pi$ $[O^{2+}(2s^22p^2\ ^1D)+He^+(1s\ ^2S)]$ | 2.54635 | 2.51356 | 0.0328 |
| 3 $^2\Pi$ $[O^{2+}(2s2p^3\ ^3D^o)+He^+\ (1s\ ^2S)]$ | 14.83085 | 14.8832 | 0.0524 |
| 4 $^2\Pi$ $[O^{2+}(2s2p^3\ ^3P^o)+He^+\ (1s\ ^2S)]$ | 17.63092 | 17.6532 | 0.0223 |
| 5 $^2\Pi$ $[O^+(2s^22p^3\ ^2D^o)+He^{2+}\ ]$ | 22.75189 | 22.6218 | 0.1301 |
| 6 $^2\Pi$ $[O^{2+}(2s2p^3\ ^1D^o)+He^+\ (1s\ ^2S)]$ | 23.22529 | 23.19174 | 0.0336 |
| 7 $^2\Pi$ $[O^+(2s^22p^3\ ^2P^o)+He^{2+}]$ | 24.46294 | 24.314 | 0.1489 |
| 8 $^2\Pi$ $[O^{2+}(2s2p^3\ ^1P^o)+He^+\ (1s\ ^2S)]$ | 26.16208 | 26.09394 | 0.0681 |
| 9 $^2\Pi$ $[O^{3+}(2s^22p\ ^2P^o)+He(1s^2\ ^1S)]$ | 30.34771 | 30.38001 | 0.0323 |
| 10 $^2\Pi$ $[O^{2+}(2s^22p3s\ ^3P^o)+He^+\ (1s\ ^2S)]$ | 33.12118 | 33.1666 | 0.0454 |

# Avoided crossing distances and energy separations for the adiabatic states of $[OHe]^{3+}$

| Molecular states | $R_x$ (units of $a_0$) | $\Delta U$ (eV) | Molecular states | $R_x$ (units of $a_0$) | $\Delta U$ (eV) |
|---|---|---|---|---|---|
| $3\,^2\Sigma^+ - 4\,^2\Sigma^+$ | 2.40 | 0.0640 | $3\,^2\Pi - 4\Pi$ | 2.70 | 0.0024 |
| $3\,^2\Sigma^+ - 4\,^2\Sigma^+$ | 4.40 | 0.0149 | $4\,^2\Pi - 5\Pi$ | 2.40 | 0.1045 |
| $4\,^2\Sigma^+ - 5\,^2\Sigma^+$ | 9.26063 | $6.46\times10^{-7}$ | $4\,^2\Pi - 5\Pi$ | 4.39 | 0.00689 |
| $5\,^2\Sigma^+ - 6\,^2\Sigma^+$ | 13.00204 | $3.80\times10^{-6}$ | $5\,^2\Pi - 6\Pi$ | 7.16306 | $7.22\times10^{-7}$ |
| | | | $6\,^2\Pi - 7\Pi$ | 7.671 | $1.156\times10^{-4}$ |
| | | | $7\,^2\Pi - 8\Pi$ | 9.25612 | $1.61\times10^{-6}$ |
| | | | $8\,^2\Pi - 9\Pi$ | 13.01033 | $1.226\times10^{-6}$ |

# Adiabatic and diabatic potentials of $[OHe]^{3+}$ ($^2\Sigma^+$)

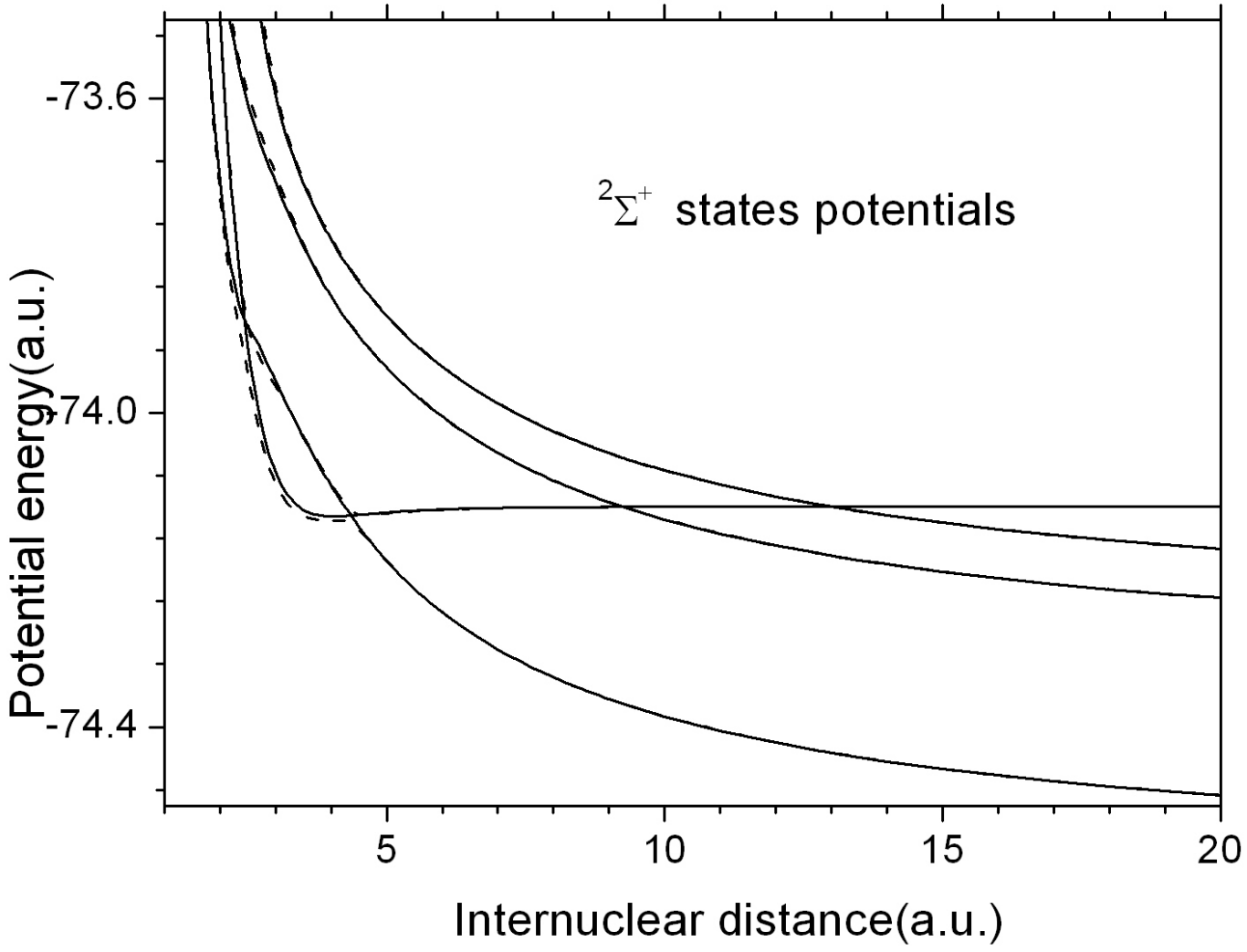

# Adiabatic radial couplings of $[OHe]^{3+}$ as a function of internuclear distance. ($^2\Sigma^+$)

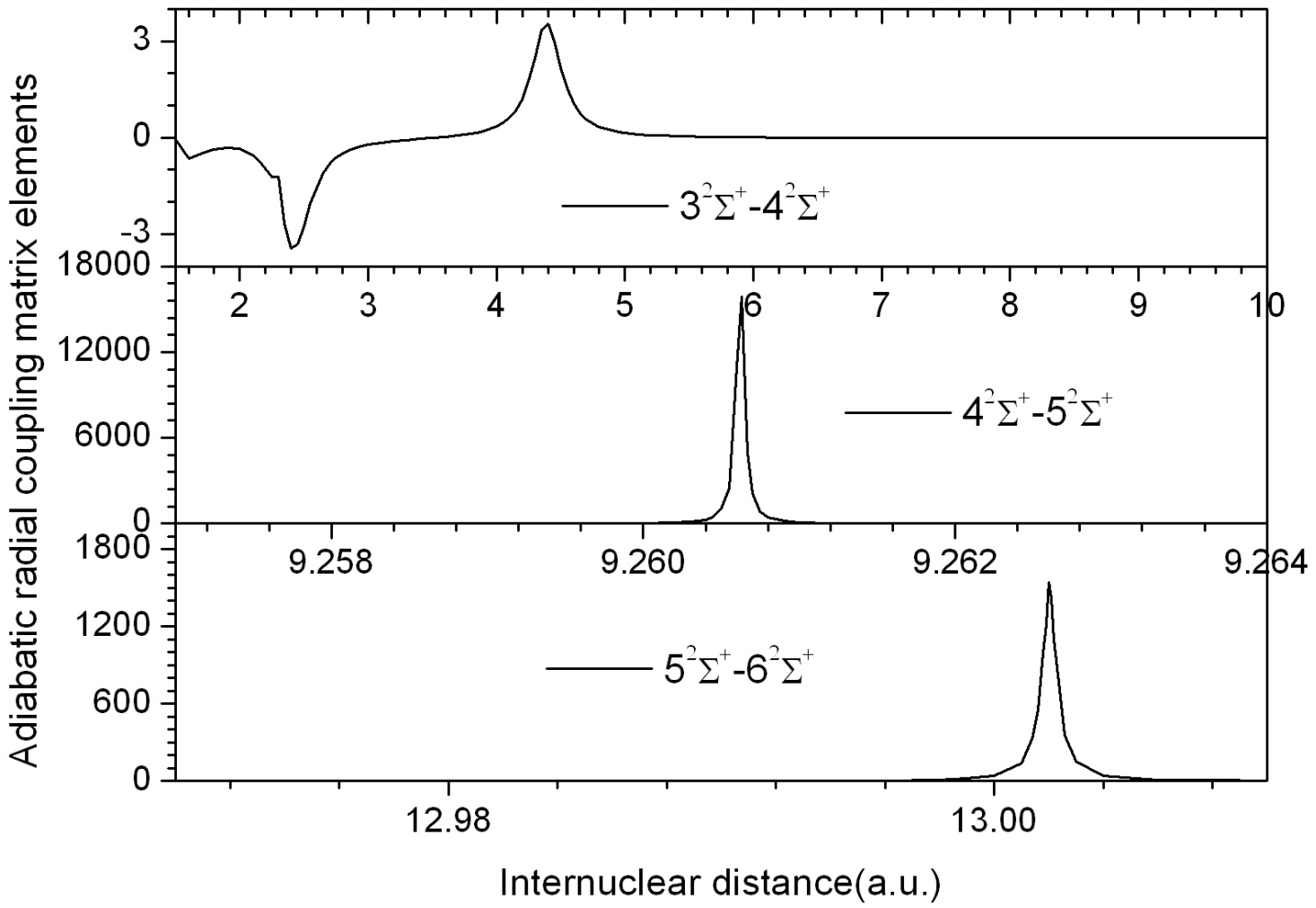

# Diabatic radial couplings of $[OHe]^{3+}$ as a function of internuclear distance. ($^2\Sigma^+$)

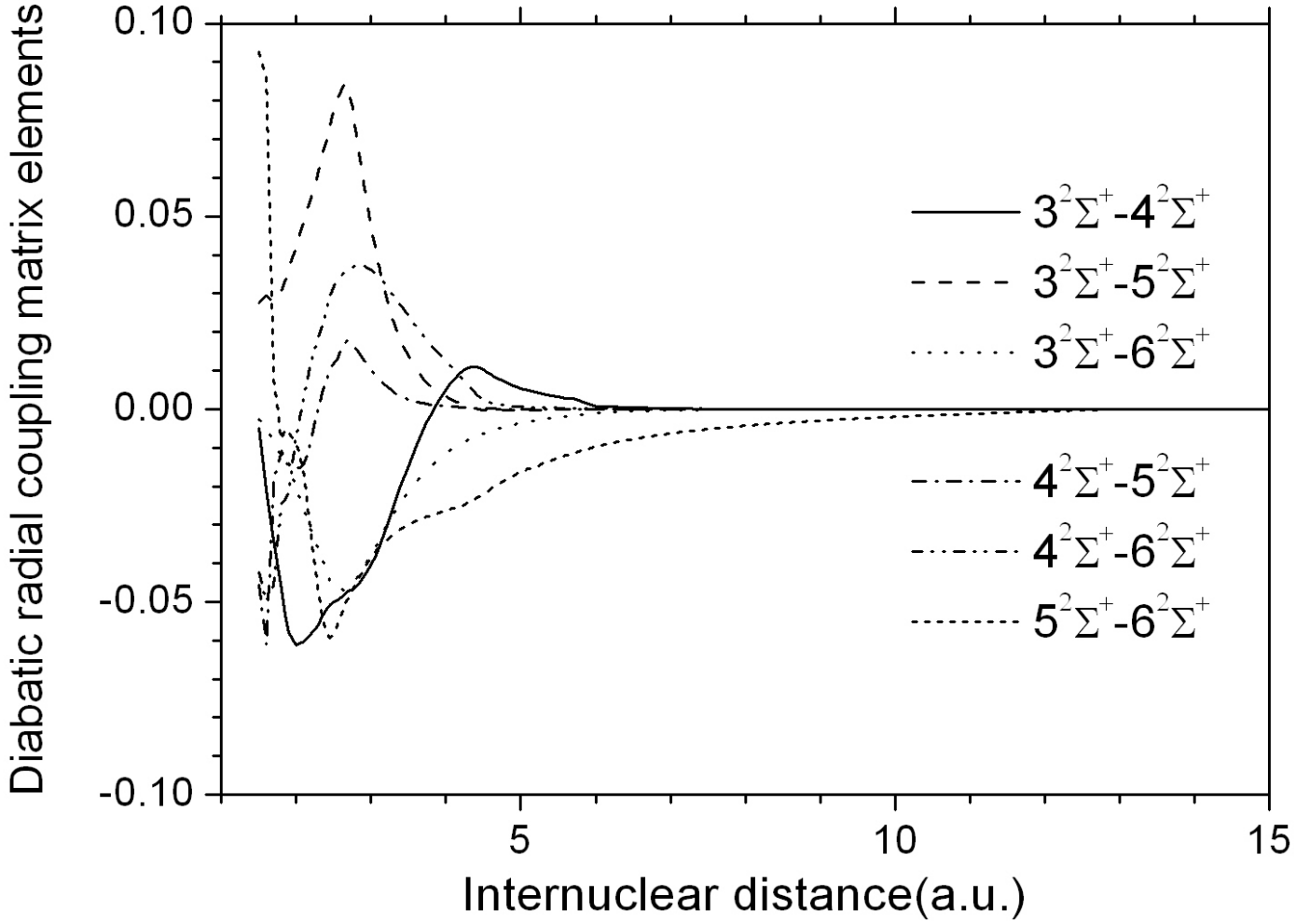

# Adiabatic and diabatic potentials of $[OHe]^{3+}$ ($^2\Pi$ )

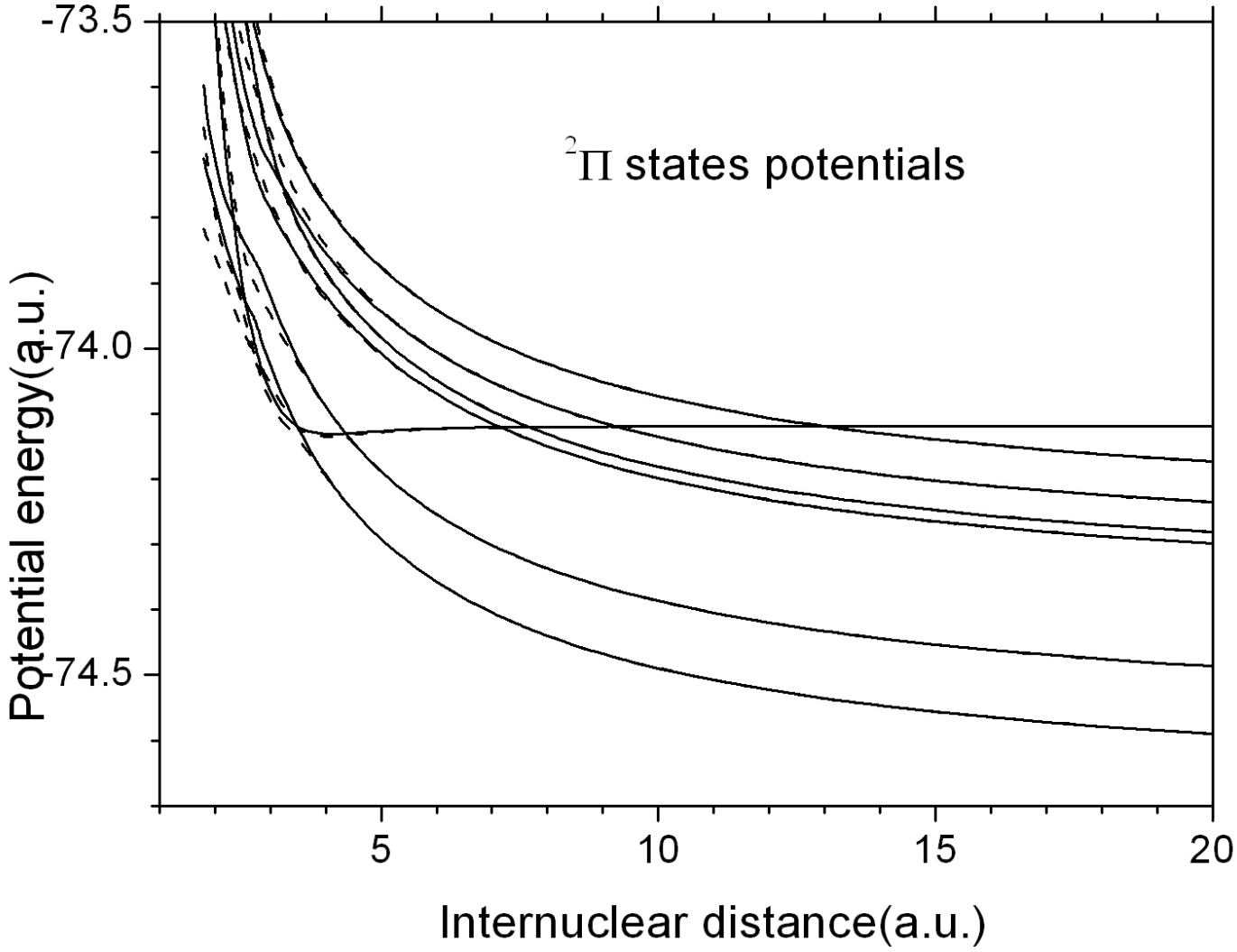

# Adiabatic radial couplings of $[OHe]^{3+}$ as a function of internuclear distance. ($^2\Pi$)

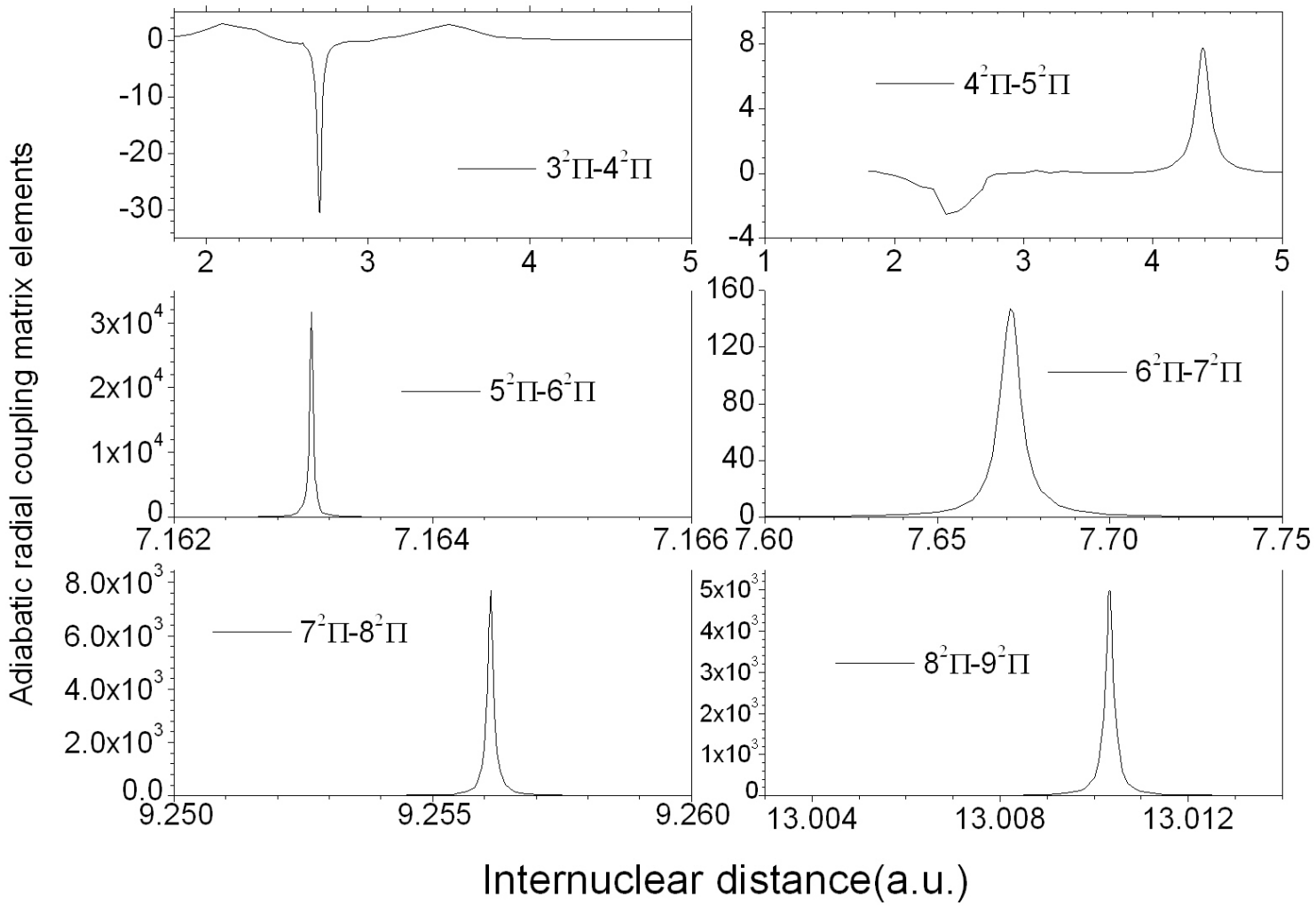

# Diabatic radial couplings of $[OHe]^{3+}$ as a function of internuclear distance. ($^2\Pi$)

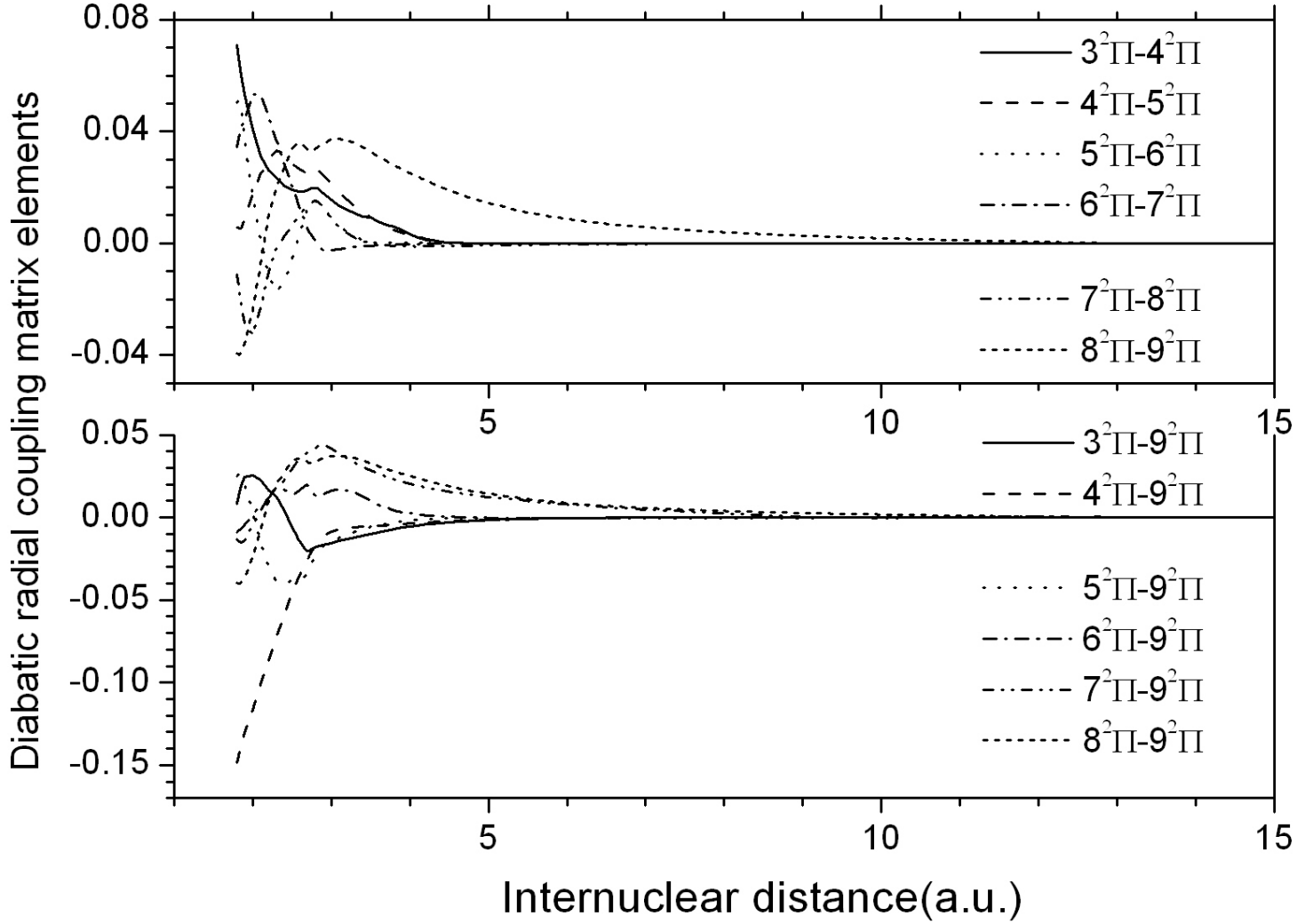

## (Ⅱ) Charge transfer cross section calculations

**The radial equations were solved by the algorithm proposed by Johnson [19] for solution of the stationary Schrödinger equation using the logarithmic derivatives for each partial wave, with $R_{max}$=*800 and with* $R_{min}$ =*0.1 a.u.*. The step $\Delta R$ *in R used on the numerical mesh was* 0.0001 a.u. for all energies.**

# Total charge transfer cross sections

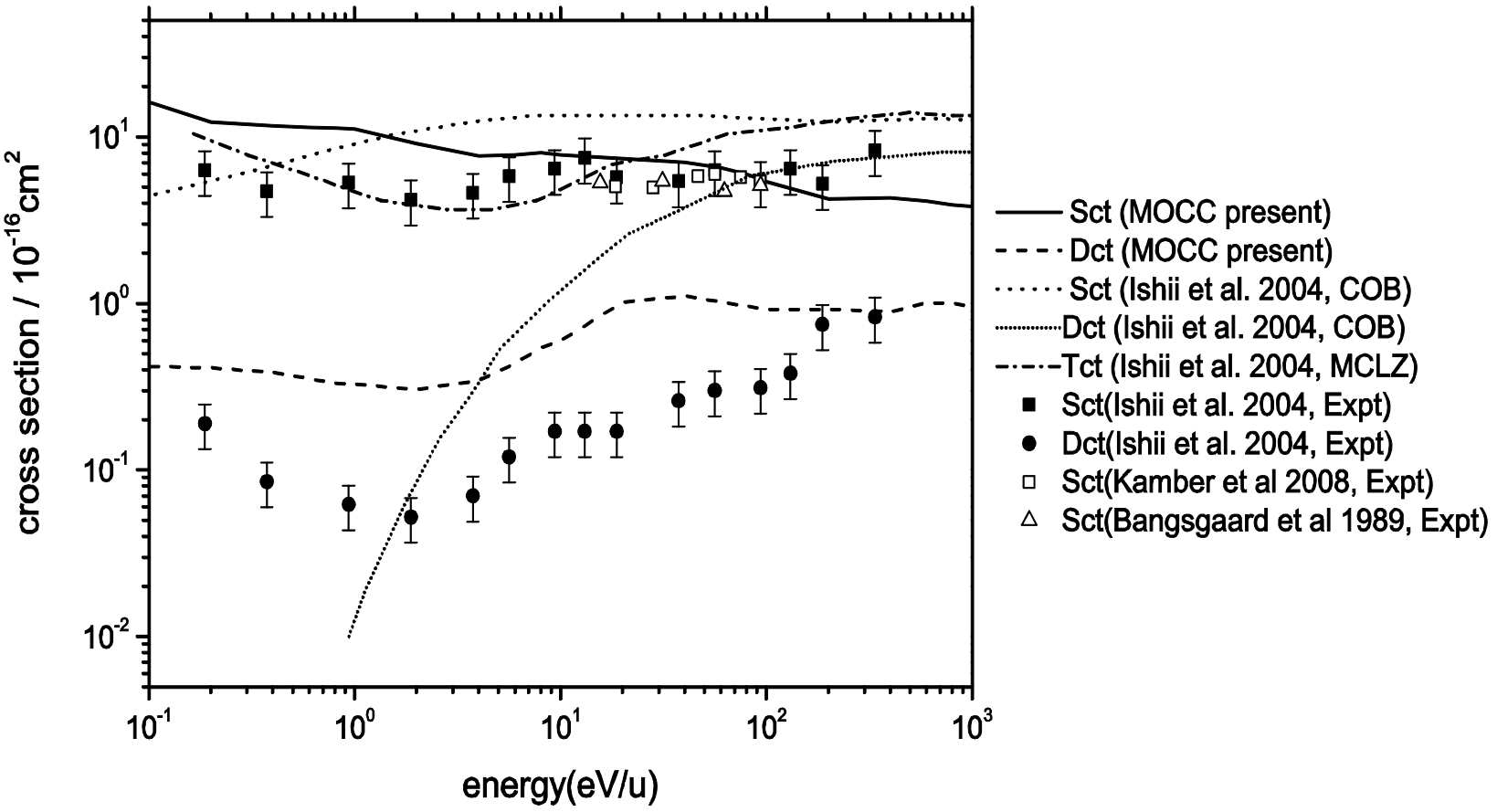


**Experiment: Low energy, angular scattering effect.**

**Acceptance angle $\theta \propto Q/(2E)$, Q: energy defect, E: incident energy**

# State-selective charge transfer cross sections

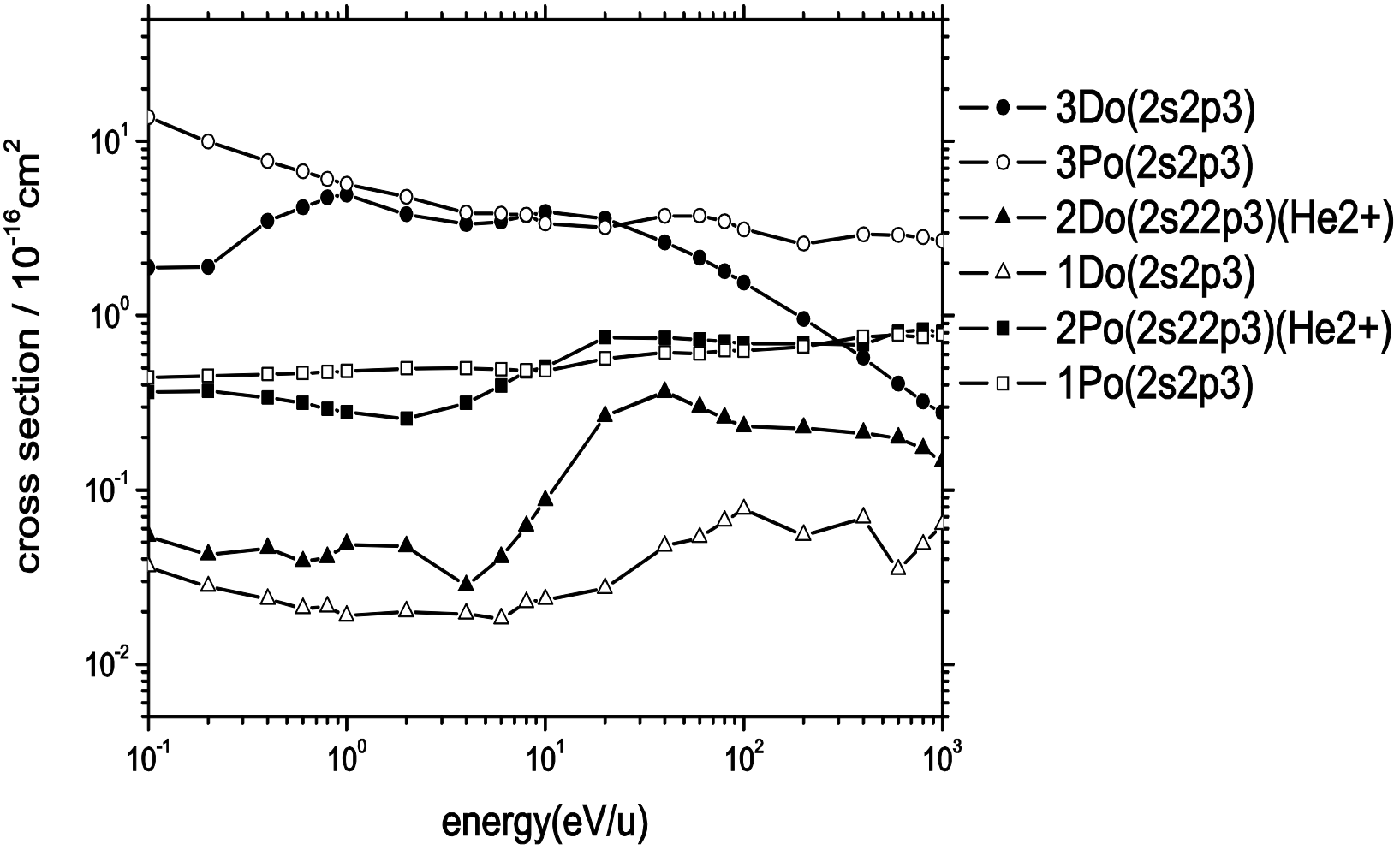

# Comparison of state-selective cross section

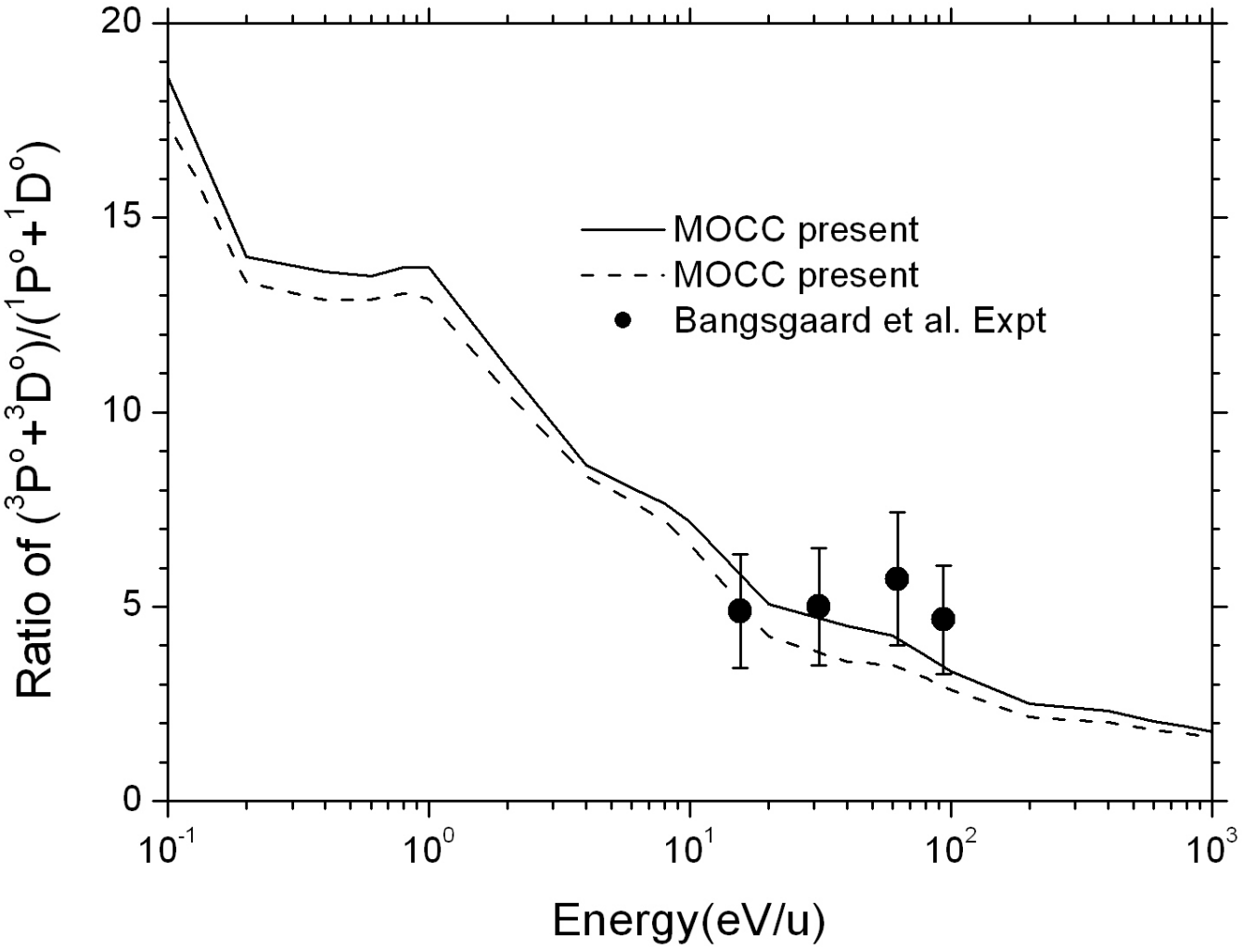

# Rate coefficient calculation:$10^2$ K-$10^5$ K

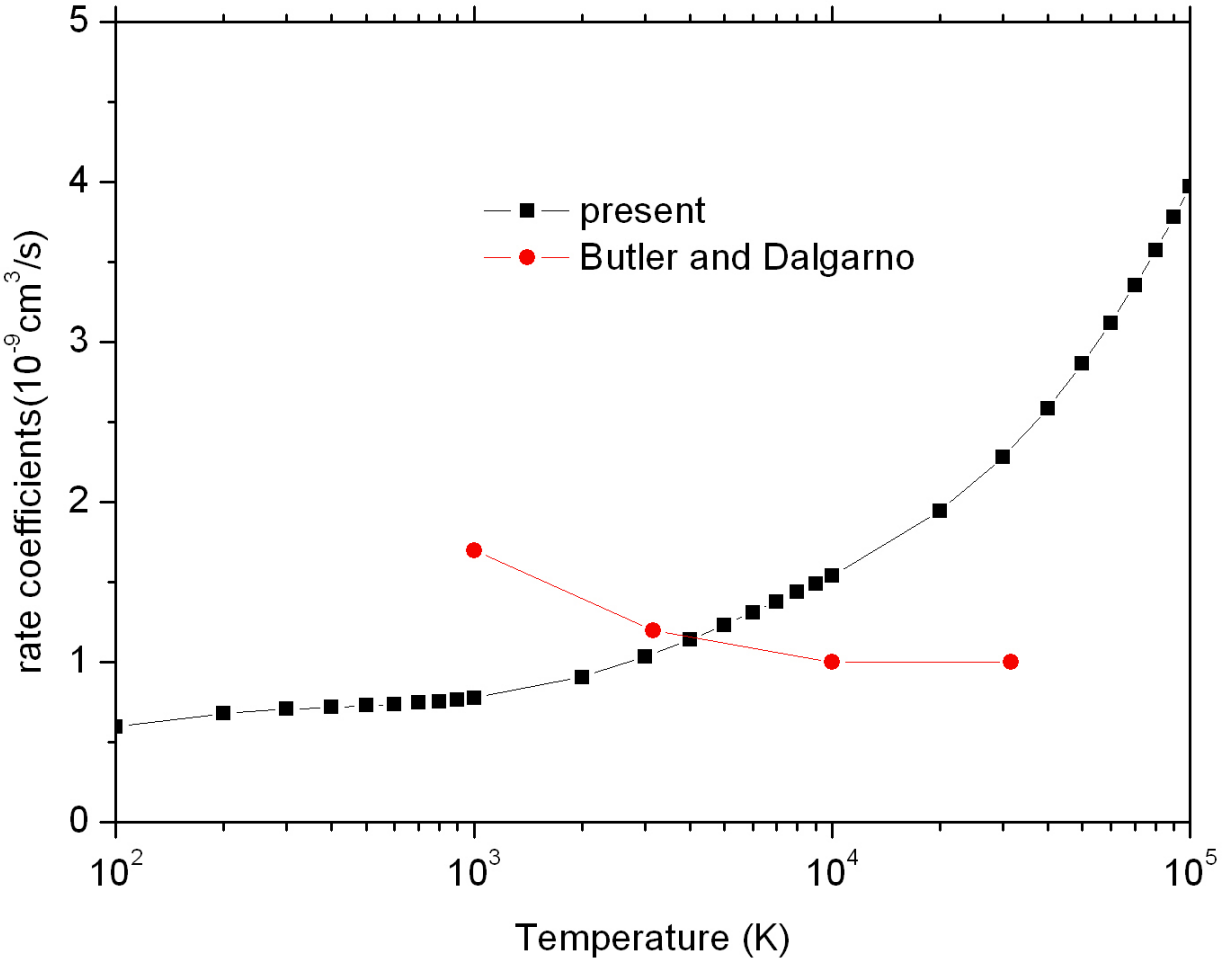


Butler, S. E. and Dalgarno, A., Astroph. J. 241, 838 (1980)

# Oscillation structures in different energy range

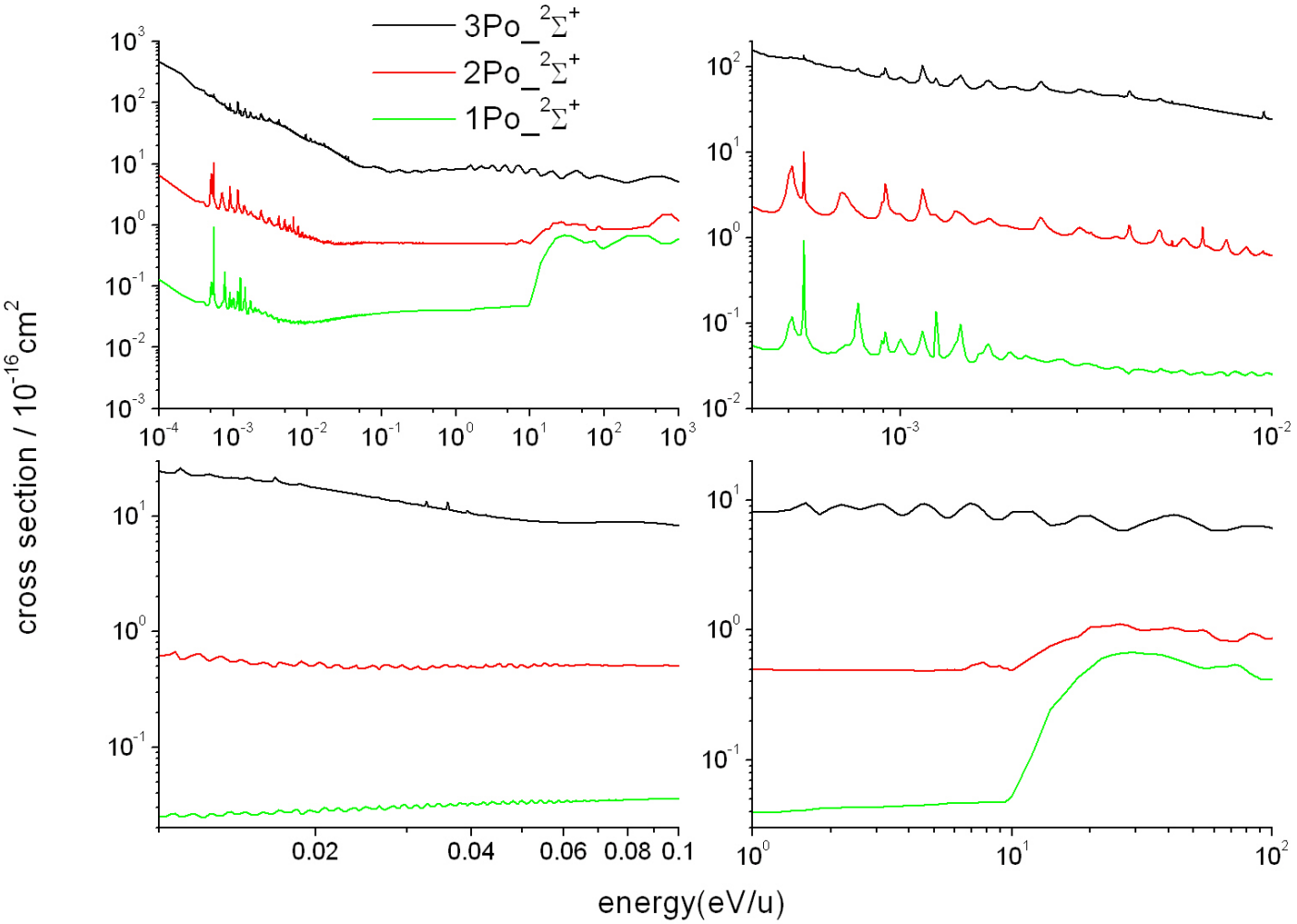


**Previous:**

**(HH)+**
**(LiH)+**
**(BeH)+**
**(BH)+**

**Oscillation structure for the nonresonant charge exchange process, highly charge ion!**
**E<1eV: Shape resonances, Regge oscillations; E>1eV: glory oscillations**

# Formation of shape resonances

$$E_\gamma = \varepsilon_\gamma^{\,d}(R) + L(L+1)/2\mu R^2$$

**Adiabatic potential plus the orbital centrifugal term**

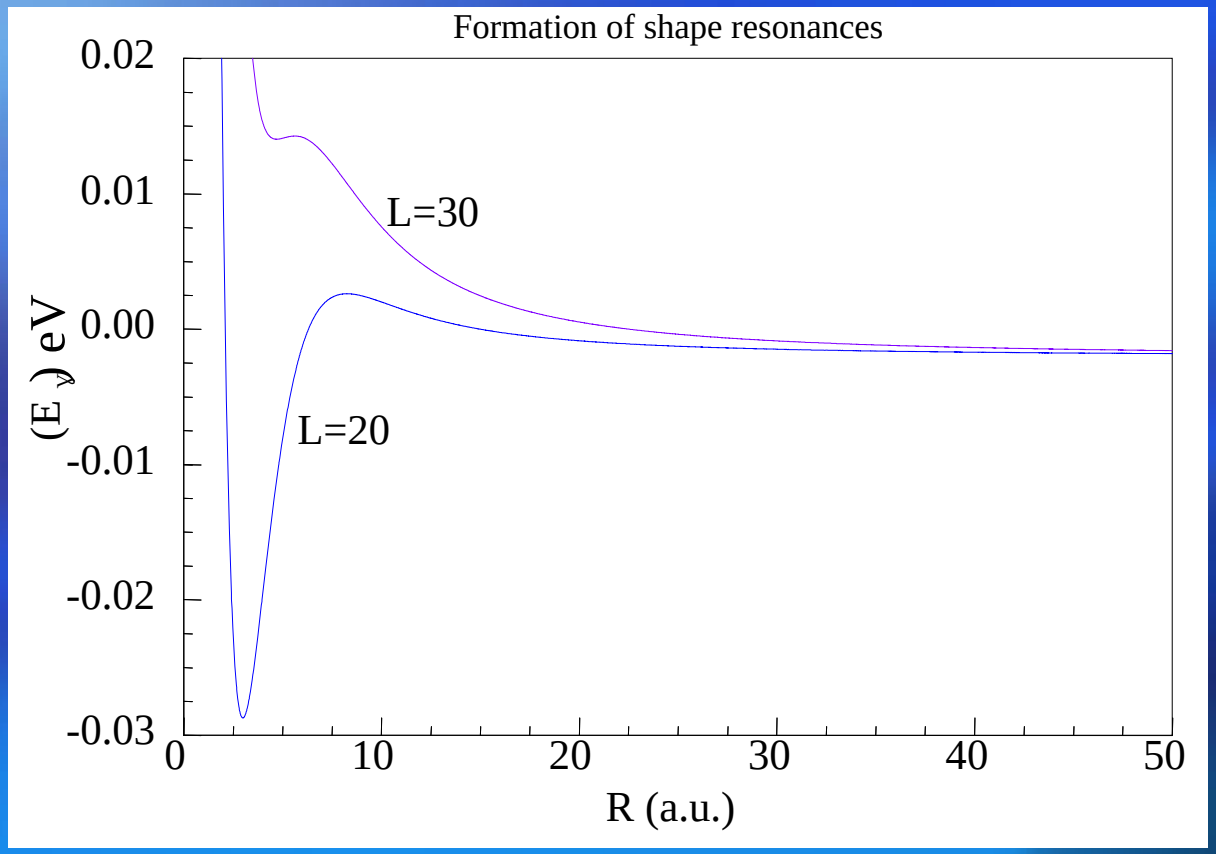


***Shape resonances arise from individual partial waves!***

**Regge oscillations:** caused by the Regge poles (when cross section is considered as a function of a partial wave angular number L, and L is expanded to the complex plane, the poles in the L plane are Regge poles)

***Determine the pole of the S-matrix in the complex L plane***

$$S_L = S_L^{\mathrm{WKB}} e^{4i\phi_0} \frac{1 + Ae^{-2i\phi_2 - 2i\phi_0}}{1 + Ae^{2i\phi_2 + 2i\phi_0}}.$$

$$\phi_2 = \int_{R_0}^{R_1} \sqrt{q(R')}\, dR',$$

$$q(R) = 2\mu[E - V_{\mathrm{eff}}(R)],$$

$$V_{\mathrm{eff}}(R) = V(R) + \frac{(L+1/2)^2}{2\mu R^2},$$

$$\phi_0 = \frac{1}{2}\arg\Gamma\left(\frac{1}{2} + ia\right) + \frac{a}{2}(1 - \ln\langle a\rangle),$$

$$S = \exp(i2\eta_L)$$

$$A = 1/\sqrt{1 + e^{-2\pi a}},$$

$$a = \frac{1}{\pi}\int_{R_1}^{R_2} \sqrt{-q(R')}\, dR',$$

See details in P. S. Krstic, et al 2004, Phys. Rev. A, 70, 042711; 2004, PRL, 183203.

# *Glory oscillations (not associated to a single partial wave)*

**Bernsten, Adv. Chem. Phys. 10, 75 (1966):**
**"Sum over $\sin^2 \eta_L$ may oscillate if $d\eta_L/dL$ vanishes",** ***glory***

**Glory oscillations:**
**Semiclassical effect, Interactions between different partial wave.**
**The partial cross sections, as a function of orbital angular momentum are oscillating functions of L, giving the biggest contribution for that L around a point of stationary phase (in L). This point depends on the collision energy. As a consequence, due to the moving point of stationary phase with L (which is the main contribution to the cross section, in sum over L), one can see the oscillations in the total cross section.**

# Summary:

1, *Ab initio adiabatic potential and radial coupling for* $O^{3+}$+He system are calculated.

2, Total and state-selective cross section of electron capture cross section for collisions energies from 0.0001eV/u - 1000eV/u are obtained. Good agreement with the experimental values is achieved.

3, Rate coefficients for $10^2$K-$10^5$K are computed and large discrepancy is found between our calculation and the previous theory.

4, Resonance structure for the nonresonant charge exchange process (rather than for the elastic cross sections) for a highly charge ion are found for the first time.

# Perspectives：

1, MRDCI is applied to calculate the electronic structures and dynamical properties of the ground and excited states of small molecules

2, MOCC is used to study the elastic, charge transfer (including collision and radiative charge transfer processes), excitation and ionization processes in the low incident energy range. Precise data can be provided, including total and state-selective cross sections and rate coefficients.

3, Investigation of the spectroscopy emitted in the charge transfer process.

# Collaborators:

**Prof. P. Stancil, UGA, USA**

**Prof. R. J. Buenker, Yan Li, Universität Wuppertal, Germany**

**Dr. P. S. Krstic, Oak ridge, USA**

**Prof. X. Ma, Institute of Modern Physics, Chinese Academy of Sciences, China**

# Thank you for your attention !